PHYSICAL REVIEW B **81**, 140102(R) (2010)

Electric-field-induced domain switching in the charge/orbital-ordered state of manganite $La_{0.5}Sr_{1.5}MnO_4$

Y. Murakami,* S. Konno, T. Arima, and D. Shindo
Institute of Multidisciplinary Research for Advanced Materials, Tohoku University, Sendai 980-8577, Japan

T. Suzuki
JEOL Ltd., Akishima 196-8558, Japan

(Received 27 January 2010; revised manuscript received 16 February 2010; published 7 April 2010)

Domain switching in the charge/orbital-ordered state of $La_{0.5}Sr_{1.5}MnO_4$, which can be manipulated by applying an electric field, was studied by *in situ* transmission electron microscopy. Dark-field images revealed the formation of micrometer-scale charge/orbital-ordered domains on cooling, which were separated by a clearly defined, meandering interface. Applying a uniaxial electric field aided the growth of a domain with its orbital chain (i.e., the direction of easy electron hopping) parallel to the applied field. These observations provide useful information for understanding of the switching mechanism of charge/orbital-ordered domains in manganite.

DOI: 10.1103/PhysRevB.81.140102 PACS number(s): 75.47.Lx, 68.37.Lp, 71.30.+h, 75.70.Kw

I. INTRODUCTION

Hole-doped manganites have attracted considerable attention in the last decade because they exhibit colossal magnetoresistance (CMR, a dramatic decrease in resistivity caused by applied magnetic fields).[1] CMR occurs because an applied magnetic field stabilizes the ferromagnetic metal phase relative to the competing phase, a charge/orbital-ordered (COO) insulator phase.[1–3] The latter phase is characterized by a regular array of manganese ions (Mn^{3+} and Mn^{4+}) and alignment of e_g orbitals at the Mn^{3+} site as shown in Fig. 1. The phase stability can also be influenced by other stimuli such as an electric field.[4] In fact, several research groups have demonstrated the occurrence of an electric-field-induced (or electric-current-induced) phase transition from the COO phase to the ferromagnetic phase.[5–10] In recent manganite investigations, researchers have been highly interested in switching COO domains by applying an electric field.[11–14] For example, the layered manganite $La_{0.5}Sr_{1.5}MnO_4$, which has tetragonal symmetry ($I4/mmm$) at room temperature, produces two kinds of COO domains on cooling[14,15] (see Fig. 1). These two COO domains (which exhibit a small orthorhombic distortion[16]) can be distinguished by the orientation of the "chains" and "stripes" of the e_g orbital of Mn^{3+} ions, as illustrated in Fig. 1. Since this ordering generates significant optical/magnetic anisotropy in the COO domains, manipulation of domains by an electric field will be essential for applications of hole-doped manganites in optoelectric devices. However, observations in previous studies on domain switching were all conducted by polarized optical microscopy. We expect that transmission electron microscopy (TEM) observations will provide further information regarding the underlying mechanisms because of their higher resolutions and the effective combination of imaging and diffraction. In this Rapid Communication, we report the results of *in situ* TEM observations of electric-field-induced switching of COO domains in $La_{0.5}Sr_{1.5}MnO_4$ as well as the evolution of COO portions upon cooling.

II. EXPERIMENTAL PROCEDURE

A single crystal of $La_{0.5}Sr_{1.5}MnO_4$ was fabricated by the floating zone method. We developed the following specimen preparation process for *in situ* TEM observations using a JIB-4600 focused ion-beam (FIB) system and manipulators. A block (approximately $15\times10\times5$ μm^3) was cut from the crystal and fixed on the surface of a Mo plate using an insulating epoxy resin. To enhance the electrical conduction between the specimen and the Mo plate, a rectangular portion together with its interface was removed using the FIB and the vacant space was filled with W (as an electrode) using a spot deposition tool, as shown in Fig. 2(a). Another W electrode was formed on the top of the crystal. A polished terminal of Au wire was connected to the upper electrode using the manipulator and W deposition. The central area of the crystal was then thin-foiled by the FIB, as shown in the scanning ion microscopy image of Fig. 2(b). The thin-foil area (approximately $6\times8\times0.1$ μm^3), which was sandwiched between the W electrodes, was used for detailed

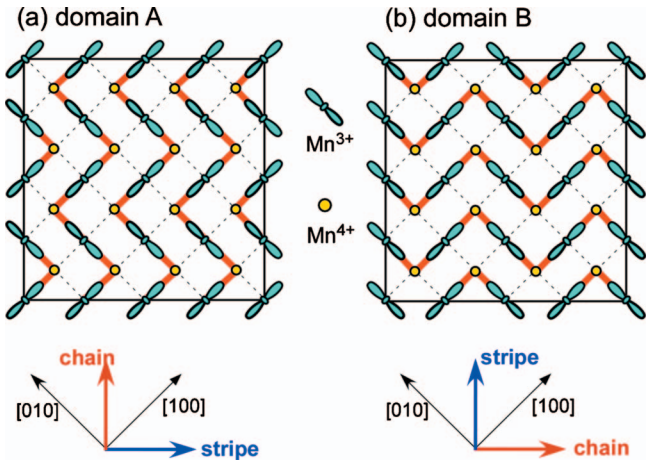

FIG. 1. (Color) Schematic illustration of the COO state in $La_{0.5}Sr_{1.5}MnO_4$. Red solid lines indicate the orbital chain whose direction defines two types of domains: A and B.

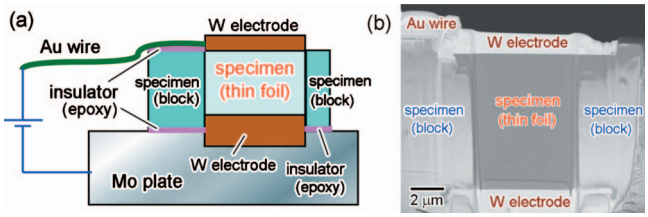

FIG. 2. (Color) Specimens used in the TEM study. (a) Schematic illustration of the specimen to which tungsten (W) electrodes and gold (Au) wires were attached to manipulate the COO domains by applying an electric field. (b) Scanning ion microscopy image of the thin-foiled area.

TEM observations. This assembly was placed on a liquid nitrogen cooling stage with electric terminals (Gatan/Oxford HC3500). The Au wire and the Mo plate were, respectively, connected to the anode and cathode using silver paste. Thus, a nearly homogeneous electric field could be applied to the thin-foil area at low temperatures. TEM observations were performed using a 200 kV electron microscope (JEM-2010 Ω). After electron-diffraction measurements, the critical temperature at which charge/orbital ordering occurred was approximately 220 K, which is consistent with resistivity measurements by Moritomo *et al.*[15] (we denote this critical temperature of charge/orbital ordering by "T_{COO}" in the subsequent sections).

III. RESULTS AND DISCUSSION

A thin-foil specimen had micrometer-scale COO domains below T_{COO}, as shown in Figs. 3(a) and 3(b). These dark-field images were obtained using the superlattice reflections indicated by the arrows in the insets. The upper bright area in Fig. 3(a) represents a COO domain whose orbital chain is parallel to [110]. We refer to this domain as "domain A" based on the illustrations in Fig. 1. The lower part in the foil was occupied by "domain B," which has its orbital chain aligned to $[1\bar{1}0]$ [Fig. 3(b)]. Both COO domains show a mottled contrast due to local imperfections in the charge/orbital ordering, which is reminiscent of antiphase boundaries observed in ordered alloys and compounds.[17–19] Thus, the dark-field images reveal two internal structures with different length scales: (1) micrometer-scale COO domains that are characterized by their orbital chain orientation and (2) submicrometer-scale dots observed in each COO domain (i.e., the mottled contrast in dark-field images). In this section, we briefly discuss the formation of the submicrometer-scale dots on cooling. Subsequently, we discuss manipulation of the micrometer-scale COO domains by an electric field.

Figures 3(d)–3(i) show the evolution of COO portions within domain A (i.e., bright dots in dark-field images) during cooling. The approximate field of view is indicated by the red rectangle in Fig. 3(a). Although thermal drift and/or optical misalignment during cooling did not permit continuous observation of the growth of specific dots over this wide temperature range, these snapshots reveal important information on the microstructural evolution. It is difficult to identify the COO portions in Fig. 3(d) due to the significant statistical noise, but the diffraction pattern did include weak superlattice reflections at this temperature. At 183 K, nanometer-

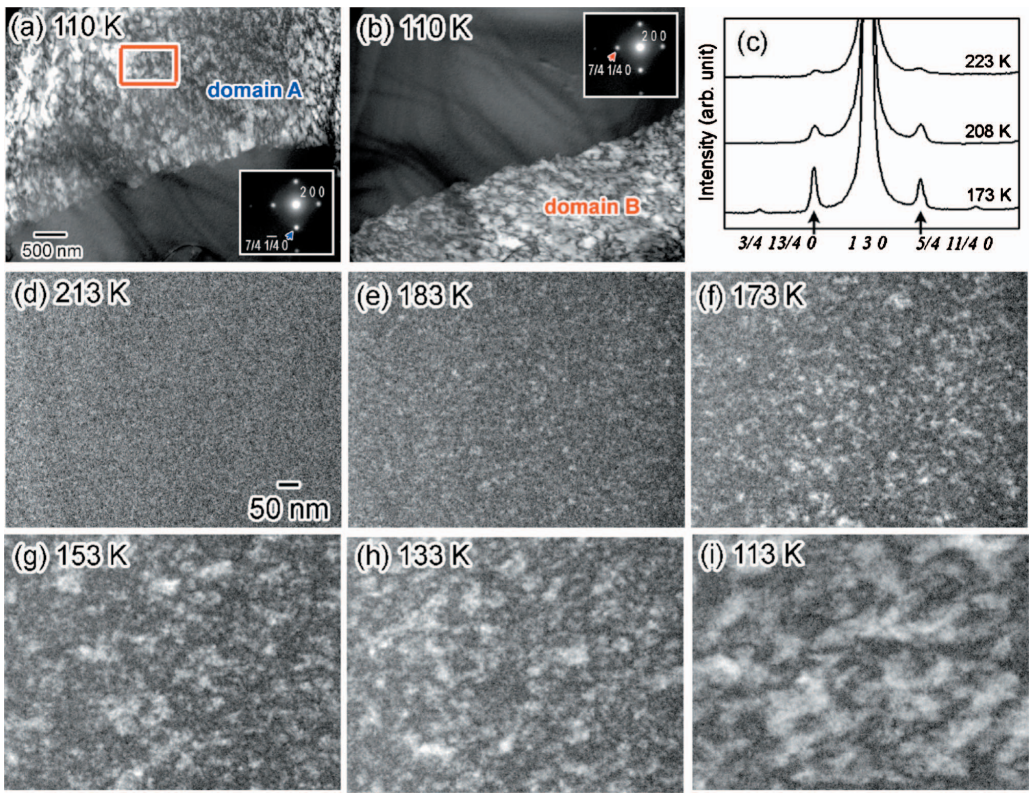

FIG. 3. (Color) Thermally induced COO domains. [(a) and (b)] Dark-field images showing micrometer-scale COO domains produced in a thin-foil specimen. (c) Intensity profile of electron-diffraction patterns. The reflections indicated by arrows are due to charge/orbital ordering. [(d)–(i)] Evolution of submicrometer-scale COO portions (observed in domain A) on cooling.

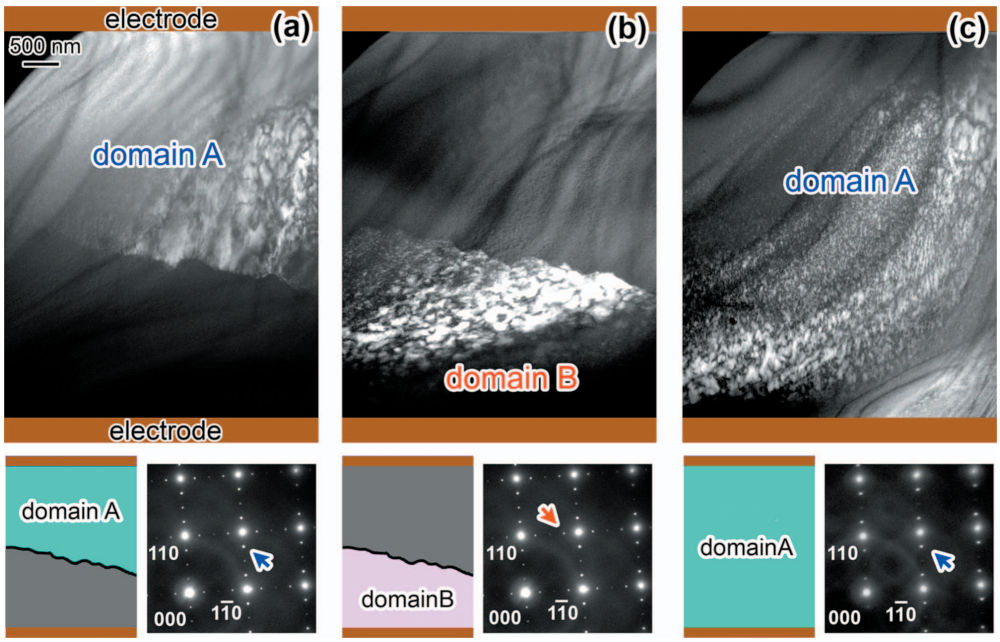

FIG. 4. (Color) Effect of the applied electric field on the COO domains. [(a) and (b)] Thermally induced COO domains observed at 110 K. (c) The domain structure caused by the applied electric field. The image in (c) was recorded at 110 K after removing the electric field. Upper panels show dark-field images. Lower panels present schematic illustrations of the observed domains (left) and the electron-diffraction patterns (right).

sized dots (i.e., COO portions) were clearly observable in the field of view. Note that, with respect to the bright dots shown in this dark-field image, the orbital chain should be aligned in the same direction (i.e., orbital chain parallel to [110]). The size of the bright dots increased on cooling, which must be due to an increase in the correlation length of charge/orbital ordering [see Figs. 3(f)–3(i)]. These observations are consistent with a gradual increase in the intensity of the superlattice reflections, as indicated by arrows in Fig. 3(c). It appears that the size of the dots at 110 K (i.e., approximately 200 nm) is comparable to the roughness of the COO domain interface, as shown in Figs. 3(a) and 3(b). The structure of the domain interface was distinct from that of the linear interface, as observed in $Bi_{1-x}Sr_xMnO_3$ (Ref. 12) and $Eu_{0.5}Ca_{1.5}MnO_4$,[13] both of which have larger orthorhombic distortions than $La_{0.5}Sr_{1.5}MnO_4$. The reason why internal structures with different length scales (i.e., micrometer-scale COO domains and submicrometer-scale dots) are produced is not clear. Nevertheless, it is interesting to note that such a hierarchical structure has also been observed in the COO domains in other manganite systems,[17,18] as well as in martensite variants (i.e., ferroelastic domains) produced by a displacive phase transformation in metallic alloys.[19] We shall also remark that previous diffraction studies on perovskite-type manganites may provide useful information about the submicrometer-scale COO portions: e.g., Radaelli *et al.* ($La_{0.5}Ca_{0.5}MnO_3$, Ref. 20) and Jirák *et al.* ($Pr_{0.5}Ca_{0.5}MnO_3$, Ref. 21). They claimed the presence of discommensurations which separated perfectly ordered regions in the COO phase. The faulting such that shown in Figs. 3(a) and 3(b) (i.e., a contrast indicative of antiphase boundaries) may have a character as discommensurations. Although our TEM observations have demonstrated the evolution of COO portions upon cooling, a careful study of discommensurations (e.g., temperature dependence of their density and/or location) may promote our understanding of the nature of hierarchical COO structure: this is indeed a challenging problem for future studies.

Next, we discuss the effects of an applied electric field on the COO domains. This experiment was performed using a different thin-foil specimen from that shown in Fig. 3. On cooling in a negligible electric field, the specimen produced two micrometer-scale domains in the viewing field: domain A (upper portion) and domain B (lower portion) as shown in Figs. 4(a) and 4(b), respectively. The arrows in the lower panels indicate the reflections used to form the dark-field images. When an electric field (2×10^4 kV/cm) was applied to the specimen at 110 K, domain B vanished completely, while domain A dominated the thin-foil area, as shown in Fig. 4(c). The dark-field method excited only limited portions of the micrometer-scale domains due to the variation of diffraction conditions within the bending foil. Nevertheless, Fig. 4(c) demonstrates the disappearance of the wavy interface that separated the thermally induced domains A and B. Furthermore, the electron-diffraction pattern [lower panel in Fig. 4(c)] exhibits superlattice reflections related to domain A only. Note that the diffraction pattern in Fig. 4(c) was recorded after the applied electric field had been removed. This observation indicates that the single-domain state is retained even after the electric field has been turned off. When the specimen was subjected to another thermal cycle (heating to room temperature and then cooling to T_{COO}), a multiple-domain state such as that in Figs. 4(a) and 4(b) was again observed.

The observations in Fig. 4 reveal that an electric field can influence the structure of COO domains in $La_{0.5}Sr_{1.5}MnO_4$.

In particular, in this experiment, a uniaxial electric field increased the volume fraction of the COO domain with its orbital chain parallel to the field direction. According to a theoretical study of in-plane anisotropy in manganites,[16] hopping of e_g electrons along the orbital chain should be easier than their transfer along the orbital stripe. This prediction is consistent with our observations, which indicate that a close relationship exists between charge delocalization and domain switching. The results also agree with anisotropy studies of the COO state in $Bi_{1-x}Sr_xMnO_3$ ($x \approx 0.5$) (Ref. 12) and $Eu_{0.5}Ca_{1.5}MnO_4$,[13] which reported an increase in the COO domain volume with a high-conductivity axis parallel to the applied electric field.

Recently, Konno *et al.*[14] carried out an intensive study of the COO state in $La_{0.5}Sr_{1.5}MnO_4$ using polarized optical microscopy. They supplied a relatively large current (of the order of 10^2 A/cm^2) at 190 K (30 K below T_{COO}) to melt the COO state by Joule heating and subsequently reduced the electric current gradually to regain the COO domains. Interestingly, their field cooling helped form a COO domain whose *orbital stripe* (not *orbital chain*) was parallel to the electric field. This discrepancy may be due to differences in the experimental conditions. We applied a large electric field (2×10^4 kV/cm) to the specimen at 110 K (110 K below T_{COO}), at which the resistivity was over 10^5 Ω cm. In fact, the electric current was too low to measure accurately, being below 10 nA (2 A/cm^2). Under these experimental conditions, we were unable to clearly observe the melting process of the COO phase when the domain switching shown in Fig. 4 occurred. Domain switching is probably affected by several factors besides the direct contribution of the electric current. For example, in our experiment with a limited current, we should consider the electrostatic energy stored in individual domains. Provided that a COO domain has an anisotropic electric permeability ε, which is related to the mobility of electrons, the electrostatic energy (which is proportional to εE^2) in a uniaxial electric field E will vary between domains. Such an energy difference may provide a driving force to grow the energetically favored domain at the expense of the energetically unfavorable one. However, further experimental and theoretical investigations of manganite are required to elucidate the reasons for its anisotropic electric permeability. The effect of mechanical stress in the thin film is another factor to consider. Nevertheless, our observations provide important information for device applications that use manganites and will help deepen our understanding of the mechanism about domain switching.

IV. SUMMARY

In summary, we performed TEM studies to reveal the internal structure of the COO phase, its formation process during cooling, and the effect of an applied electric field on the domain configuration in $La_{0.5}Sr_{1.5}MnO_4$. Thin foil specimens produced micrometer-scale COO domains on cooling, which are separated by a well-defined but meandering interface. *In situ* TEM observations demonstrated that an applied electric field helped expand a COO domain with its orbital chain oriented in the field direction. Our observations indicate that domain switching may be affected not only by an anisotropic electric current, but also by other factors such as dielectric anisotropy in the COO state.

ACKNOWLEDGMENT

This study was supported by Grants-in-Aid for Scientific Research from the Japan Society for the Promotion of Science.

*Author to whom correspondence should be addressed; murakami@tagen.tohoku.ac.jp

[1] Y. Tokura, *Colossal Magnetoresistive Oxides* (Gordon and Breach Science Publishers, Amsterdam, 2000).
[2] E. Dagotto, *Nanoscale Phase Separation and Colossal Magnetoresistance* (Springer-Verlag, Berlin, 2003).
[3] N. Mathur and P. Littlewood, Phys. Today **56**(1), 25 (2003).
[4] A. Asamitsu, Y. Tomioka, H. Kuwahara, and Y. Tokura, Nature (London) **388**, 50 (1997).
[5] C. N. R. Rao, A. R. Raju, V. Ponnambalam, S. Parashar, and N. Kumar, Phys. Rev. B **61**, 594 (2000).
[6] S. Srivastava, N. K. Pandey, P. Padhan, and R. C. Budhani, Phys. Rev. B **62**, 13868 (2000).
[7] Q. Liu, N. J. Wu, and A. Ignatiev, Appl. Phys. Lett. **76**, 2749 (2000).
[8] Y. Q. Ma, W. H. Song, J. M. Dai, R. L. Zhang, J. Yang, B. C. Zhao, Z. G. Sheng, W. J. Lu, J. J. Du, and Y. P. Sun, Phys. Rev. B **70**, 054413 (2004).
[9] A. Odagawa, H. Sato, I. H. Inoue, H. Akoh, M. Kawasaki, Y. Tokura, T. Kanno, and H. Adachi, Phys. Rev. B **70**, 224403 (2004).
[10] A. S. Carneiro, R. F. Jardim, and F. C. Fonseca, Phys. Rev. B **73**, 012410 (2006).
[11] K. Hatsuda, T. Kimura, and Y. Tokura, Appl. Phys. Lett. **83**, 3329 (2003).
[12] K. Taniguchi, S. Nishiyama, T. Arima, S. Konno, S. Yamada, and E. Sugano, Appl. Phys. Lett. **90**, 153501 (2007).
[13] Y. Tokunaga, R. Kumai, N. Takeshita, Y. Kaneko, J. P. He, T. Arima, and Y. Tokura, Phys. Rev. B **78**, 155105 (2008).
[14] S. Konno, K. Taniguchi, H. Sagayama, and T. Arima, Appl. Phys. Express **2**, 033004 (2009).
[15] Y. Moritomo, Y. Tomioka, A. Asamitsu, Y. Tokura, and Y. Matsui, Phys. Rev. B **51**, 3297 (1995).
[16] Y. S. Lee, S. Onoda, T. Arima, Y. Tokunaga, J. P. He, Y. Kaneko, N. Nagaosa, and Y. Tokura, Phys. Rev. Lett. **97**, 077203 (2006).
[17] Y. Murakami, H. Kasai, J. J. Kim, S. Mamishin, D. Shindo, S. Mori, and A. Tonomura, Nat. Nanotechnol. **5**, 37 (2010).
[18] M. Uehara, S. Mori, C. H. Chen, and S.-W. Cheong, Nature (London) **399**, 560 (1999).
[19] Y. Murakami and D. Shindo, Philos. Mag. Lett. **81**, 631 (2001).
[20] P. G. Radaelli, D. E. Cox, M. Marezio, and S.-W. Cheong, Phys. Rev. B **55**, 3015 (1997).
[21] Z. Jirák, F. Damay, M. Hervieu, C. Martin, B. Raveau, G. André, and F. Bourée, Phys. Rev. B **61**, 1181 (2000).